A Comprehensive Spectroscopic Study of the Polymorphs of Diflunisal and their Phase Transformations

Anuradha R. Pallipurath,[†,‡] Francesco Civati,[†] Juraj Sibik,[§] Clare Crowley,[‖] J. Axel Zeitler,[§] Patrick McArdle*[,†] and Andrea Erxleben*[,†]

[†] School of Chemistry, National University of Ireland, Galway, Ireland

[‡] Department of Chemistry, University of Bath, Claverton Down, Bath BA2 1AY, UK

[§] Department of Chemical Engineering and Biotechnology, Pembroke Street, Cambridge CB2 3RA, UK

[‖] Materials and Surface Science Institute, Department of Chemical and Environmental Sciences, University of Limerick, Ireland

*Corresponding author email address: andrea.erxleben@nuigalway.ie (AE); p.mcardle@nuigalway.ie (PM)

Abstract

Understanding phase transitions in pharmaceutical materials is of vital importance for drug manufacturing, processing and storage. In this paper we have carried out comprehensive high-resolution spectroscopic studies on the polymorphs of the non-steroidal anti-inflammatory drug diflunisal that has four known polymorphs, forms I – IV (FI – FIV), three of which have known crystal structures. Phase transformations during milling, heating, melt-quenching and exposure to high relative humidity were investigated using Raman and terahertz spectroscopy in combination with differential scanning calorimetry and X-ray powder diffraction. The observed phase transformations indicate the stability order FIII > FI > FII, FIV. Furthermore, crystallization experiments from the gas phase and from solution by fast evaporation of different solvents were carried out. Fast evaporation of an ethanolic solution below 70 °C was identified as a reliable and convenient method to obtain the somewhat elusive FII in bulk quantities.

Keywords

Diflunisal, Phase transformation, Polymorphs, Terahertz spectroscopy

Chemical Compounds

Diflunisal (PubChem CID: 3059 **)**

1. Introduction

The existence of different polymorphic forms of drugs has led to major investment and efforts into the discovery and study of polymorphs.(Dharmendra Singhal, 2004; Lee, 2014) During drug manufacturing an active pharmaceutical ingredient (API) undergoes various different processes and is subjected to different temperatures, pressures and relative humidities. (Yihong Qiu, 2009) It is hence vital to understand any polymorphic transformation that a drug substance undergoes under different conditions. Understanding crystallization kinetics under various conditions will clarify the processes which underpin polymorphic transformations that can play an important role in the activity and stability of drugs.

Traditional solution crystallization experiments can be controlled by adjusting the temperature and concentration of the system. (Coquerel, 2014) In a liquid phase, the use of higher crystallization temperatures can lead to the most thermodynamically stable polymorphic form. (Hao et al., 2012) Sublimation(Kamali, Erxleben, & McArdle, 2016) and melt quenching(Patterson JE et al., 2005) are solvent free techniques that can be used for purification and for the production of amorphous drug forms, respectively. Furthermore, polymorph seeds for bulk crystallization can be obtained by sublimation and melt quenching. It has been shown recently that templating can be applied to selectively grow polymorphs by sublimation(Kamali et al., 2016),(Srirambhatla, Guo, Price, & Florence, 2016) that otherwise gives the high temperature metastable state. (Pallipurath et al., 2015) The fast evaporation technique can provide access to kinetically controlled polymorphs. (Bag, Patni, & Reddy, 2011) ROY by Eli Lilly is one of the most interesting polymorphic compounds, having nine known forms. The presence of these polymorphs were detected on a hot stage microscope, where they crystallized from the melt.(Shuang Chen, Ilia A. Guzei, & Yu*, 2005)

Milling is regularly employed in the pharmaceutical industry for particle size reduction. However, it can also lead to polymorphic transformations, often yielding more thermodynamically stable forms. (Macfhionnghaile et al., 2014) In contrast, cryogenic milling can provide access to metastable and amorphous forms. (Macfhionnghaile et al., 2014) This technique has the added advantage that the low temperature used makes the material more brittle and thus more millable. Small quantities of solvents added to the milling processes act as lubricants or mechanical catalysts for polymorphic transformation. (Friscic, Childs, Rizvi, & Jones, 2009) Liquid assisted grinding is a subset of solvent assisted milling techniques that are used to understand polymorphic transformation and also to screen for co-crystals. (Friscic et al., 2009)

Diflunisal is a Biopharmaceutics Classification System (BCS) class II, non-steroidal anti-inflammatory drug used in the treatment of rheumatoid arthritis. It has four known polymorphs, all of which crystallize as long, thin needles. Form I (FI) is crystallized from toluene (triclinic; unit cell parameters – 3.8, 6.77, 21.65, 82.3, 83.99, 81.98; REF code: FAFWIS01). (Cross et al., 2003) Form II (FII) is precipitated from ethanol using water as an

anti-solvent.(Brittain, Elder, Isbester, & Salerno, 2005) The single crystal structure could not be determined due to the difficulty in growing X-ray suitable single crystals of this polymorph. Form III (FIII) is crystallized from ethanol(Cross et al., 2003) and its structure was solved by Cross *et al*. through refinement of its powder pattern (orthorhombic; unit cell parameters – 39.7, 14.1, 3.83; REF code: FAFWIS02). Form IV (FIV) has a solvate channel structure and was reported by Hansen *et al*. (monoclinic; unit cell parameters – 34.66, 3.74, 20.737, β = 110.57; REF code: FAFWIS).(Hansen, Perlovich, & Brandl, 2001) The intrinsic dissolution rate was reported to follow the order IV>II>III>I, with zero order kinetics, however the order of thermodynamic stability amongst the polymorphs has not been clearly established. (Perlovich, Hansen, & Bauer-Brandl, 2002) Sung *et al*. achieved polymorph control through the use of different surfactants and microemulsion systems. (Sung, Fan, Yeh, Chen, & Chen, 2013) For example, they produced FIII using bicontinous or oil-in-water emulsions and the FIV hydrate using water-in-oil emulsion. (Sung et al., 2013) Sung *et al*. were also able to modify the size and aspect ratio of crystals using various surfactants.

In this paper, we report extensive spectroscopic studies of the phase transformations of diflunisal polymorphs. We have also identified a new technique to obtain FII in bulk that is superior to the currently used method.

2. Materials and methods

2.1 Materials

Diflunisal was purchased from Baoji Guokang Bio-Technology Co.,Ltd, China. The solvents were purchased from Sigma Aldrich and were used without further purification.

2.2 Preparation of polymorphs

FI is the commercial form and was used as received. FII was obtained by dissolving FI in ethanol and precipitating it out with water. (Brittain et al., 2005) FIII was obtained by recrystallization of FI from ethanol. (Cross et al., 2003) FIV was obtained by recrystallizing FI from a 50:50 mixture of acetone and water.(Hansen et al., 2001) The identity and phase purity of all forms was confirmed by X-ray powder diffraction.

2.3 Ball milling

Room temperature milling (RTBM) experiments were carried out in an oscillatory ball mill (Mixer Mill MM400, Retsch GmbH & Co., Germany) at 25 Hz. using a 25 mL stainless steel milling jar containing one 15-mm diameter stainless steel ball. 0.5 g of each sample was milled for 5, 15, 30, 60, 90 and 120 mins. For long milling times the jars were allowed to cool for 15 min after every 30 mins to avoid overheating.

Cryogenic milling (CBM) was carried out using the same set-up. The milling jars were initially cooled in liquid nitrogen for 5 min and subsequently for 2.5 min after every 7.5 min of milling. Polymorphs FI, FII and FIII were milled for 60 mins and 120 mins.

Liquid assisted grinding (LAG) experiments were carried out using the same set up, using 100 µL of nine different solvents, namely: water, acetone, ethanol, methanol, toluene, terahydrofuran (THF), dimethyformamide (DMF), valeric acid (VA) and chloroform. These systems were milled for 5 min, 10 min and 15 min at room temperature.

2.4 Fast evaporation

Diflunisal FI was dissolved in five different solvents: methanol, ethanol, acetone, THF and chloroform. The solvents were evaporated at 60 ºC using a rotary evaporator. For higher temperatures, up to 130 ºC, fast evaporation was achieved through heating and rapid stirring of the solution in a round bottom flask, under reduced pressure in a conventional oil bath fitted with a solvent trap.

2.5 Sublimation

Sublimation experiments were carried out in a vacuum oven as previously described,[6] under vacuum (<200 mbar, oven temperature of 80 ºC). The samples were independently heated using a microheater fitted to the sublimation area to attain a final temperature of 160 °C. Sublimation was carried out for a time interval of 24 hrs for FI and FII, and 10 hrs for FIII.

2.6 Melt quenching (QM)

All three polymorphs of diflunisal were melted on a hot plate and subsequently immersed in liquid nitrogen and used for further analysis.

2.7 X-ray powder diffraction (XRPD)

XRPD patterns of all the samples were collected with an Inel Equinox 3000 (Cu Kα, 35 kV, 25 A), between 5 and 80° (2θ) using a curved position sensitive detector calibrated using Y_2O_3. The sample holder was rotated during data collection to reduce preferred orientation effects. Calculated patterns for the polymorphs with known crystal structures can be found in the Supporting Information (SI, Figure S1).

2.8 Differential scanning calorimetry (DSC)

DSC experiments were performed on a STA625 thermal analyser from Rheometric Scientific (Piscataway, New Jersey) in open aluminum crucibles, at 10 °C/min, under nitrogen gas. Calibration was performed using an indium standard. Further DSC experiments on FII were performed on a DSC 8500 (Perkin Elmer) in sealed aluminium pans at 100 °C/min under nitrogen gas following temperature and enthalpic calibration with an indium standard.

2.9 Near infra-red spectroscopy (NIR)

NIR spectra of bulk samples (~250 mg) were collected in glass vials (15 mm × 45 mm) on a Perkin Elmer Spectrum One fitted with an NIR reflectance attachment. Spectra were collected in the range of 10000 − 4000 cm^{-1}, with a resolution of 4 cm^{-1} and 32 integrated scans.

2.10 Attenuated total reflectance infra-red spectroscopy (ATR-IR)

FT-MIR spectra were collected on a Perkin Elmer Spectrum 400 fitted with an ATR reflectance attachment. Spectra were collected in the range of 650 − 3600 cm^{-1}, with a resolution of 4 cm^{-1} and four integrated scans on a diamond/ZnSe window.

2.11 Terahertz time-domain spectroscopy (THz-TDS)

The terahertz time domain spectra were collected using the Advantest system (TAS7500TS) in the range of 0.2 to 5 THz, at a resolution of 7.6 GHz, and 8192 integrated scans. The polymorphs were highly absorbing hence they had to be diluted by geometric mixing of the samples with PTFE powder and making pellets using a 2 ton tablet press. The pellets were placed in a cuvette under vacuum (2.8 x 10^{-1} mbar). The temperature was controlled using a 50 W heater and data were acquired at 10 K intervals from room temperature up to 380 K. The absorption spectra were calculated in Matlab following a standard procedure for transmission terahertz measurements such as in reference. (Jepsen et al., 2017)

2.12 Raman spectroscopy

Raman spectra were collected using the Renishaw Invia micro-Raman spectrometer (100 – 3600 cm^{-1} range, 4 cm^{-1} resolution, 10 s exposure time, 0.5% laser power, 785 nm laser).

3. Results and Discussion

IR spectral assignments were carried out by Martinez-Oharri *et al*. (Martinez-Oharriz et al., 1999) to unravel the intermolecular hydrogen bonding interactions involved in all four forms of diflunisal before the crystal structures were available. Martinez-Oharri *et al*. concluded that FI and IV have similar interactions, while the interactions in FII resemble those in FIII. The major difference between FIV and the other forms was found for the ν(C-F) stretching bands between 1310 and 1410 cm^{-1}. We have now carried out an extensive spectroscopic analysis of all four forms, taking into account the crystal structure data that are now available.

Raman spectroscopy (**Figure 1**) shows clear differences between the four polymorphs in the phonon regions, which suggests differences in crystal structure. FI and FIV have out-of-plane stretches at 708 cm^{-1}, while FII and III have these stretches at 712 cm^{-1}. All three polymorphs have intramolecular H-bonding and the eight membered carboxylic acid dimer motif. (Cross et al., 2003) A notable similarity in all four structures is the presence of OH deformations of

monomeric COOH groups around 1270 cm^{-1} suggesting that there are free COOHs on the surface of the crystals. The major differences between the four structures are in the carbonyl regions, which are influenced by intramolecular H-bonding interactions. Three C=O stretches are observed in all polymorphs. Two of the C=O stretches occur at 1611 and 1629 cm^{-1}. These stretches are roughly 50 cm^{-1} lower in wavenumber than typically observed for carboxylic acids due to the presence of the ortho-hydroxyl group. (Socrates, 2001) The third C=O stretch indicates the extent of intramolecular H-bonding. (Socrates, 2001) FI has this band at 1685 cm^{-1}, at higher frequency than the other polymorphs. FIV has the corresponding stretch at 1665 cm^{-1} indicating the next highest degree of H-bonding, followed by FII at 1658 cm^{-1} and FIII at 1651cm^{-1}. While in all polymorphs intramolecular H-bonds and the carboxylic acid dimer are present, in FI the o-hydroxy groups of adjacent diflunisal molecules also form a four-membered ring, which in turn leads to the formation of a chain structure. (Cross et al., 2003) This feature is missing in FIII and IV as the o-hydroxy groups on the adjacent diflunisal molecules face away from each other (**Scheme 1**). A more detailed list of the spectral differences can be found in Table 1. Brittain *et al.* carried out fluorescence spectroscopy(Brittain et al., 2005) to study the differences in the electronic levels, as a result of structural differences of the polymorphs. This they attribute to the extent of interactions due to salicylate groups. FI had an emission pattern different from the others, where the double excitation bands were separated to a greater extent, which was attributed to the degree of face to face interactions of the salicylate group, with FI having no or lesser interactions than the other forms, owing to the absence of carboxylic acid dimers. This study was speculative and was carried out before the X-ray single crystal structures were determined. It is now evident that FI has a greater extent of H-bonding, with the four-membered ortho-OH group H-bonding motif and the 1D chains apart from the carboxylic acid dimers, which could be the reason for the shift in the excitation peaks.

MIR spectroscopy supports previous findings (**Figure S2**, SI), where FI is similar to FIV and FII is similar to FIII. Out-of-plane CH stretches at 895 cm^{-1} (1H, **Figure 1**), out-plane-deformation at 649 and 670 cm^{-1} (2H) in 1,2,4-substituted benzene rings and bending modes at 1376 cm^{-1} of COH in OH associated with C=O through H-bonding(Socrates, 2001) are present only in FII and III, while they are absent in FI and FIV. While there is ortho F disorder in FI and IV, FIII does not have any disordered F atoms. (Cross et al., 2003) The stretching and bending modes at 895, 649, 670 and 1376 cm^{-1} suggest the absence of disorder in FII similar to FIII. Clear differences in the out-of-plane deformations of CH and CF can be found in the region between 1877 and 1990 cm^{-1} (Table 2). The major difference in the CH…F interactions is that in FI and FIII these interactions are between the rings carrying the F atoms, while in the case of FIV they are between the rings carrying the F and the carboxyl-substituted ring of the adjacent molecule. In a previous study, we showed that the presence of a co-former in a diflunisal co-crystal prevents disorder due to the presence of CH…F

interactions between the two molecules. (Pallipurath et al., 2016) Structural differences between the polymorphs are also reflected in the NIR spectra (Figure S3 and Table S1, SI). There are some shifts in the CH-CC combination bands. Red lines in Figure S3 represent peaks that are similar in Forms II and III, while green lines are peaks that are similar in FII, III and IV. Blue lines are peaks that are similar in FI and IV, with * denoting slight shifts in peaks in FI compared to FIV.

3.1 Solution crystallization and fast evaporation techniques

Diflunisal was crystallized from various solvents by fast removal of the solvent under reduced pressure. Acetone, chloroform and THF gave FIV, while methanol gave FIII as expected. The corresponding XRPD patterns are shown in the SI (**Figure S4**). Interestingly, ethanol showed temperature dependent results. **Figure 2a** shows the XRPD patterns at intervals of 10 °C, while **Figure 2b** shows the shifting of the Raman peaks in the carbonyl region (1600 – 1700 cm^{-1}) to complement the XRPD data. While at higher temperatures no particular polymorph was reliably obtained, at temperatures between 40 and 70 °C FII was selectively produced. Usually, FII is prepared by precipitation from ethanol with water and tedious filtration of the precipitate in small portions to prevent conversion to FIII during filtration. As shown here, fast evaporation of an ethanolic solution of diflunisal below 70 °C presents a more convenient and reliable method for the preparation of bulk quantities of this polymorph.

3.2 Heating-induced phase transformations

3.2.1 Thermal analysis (TA): It is reported that all polymorphs melt at the same temperature, except for FIII that has an endotherm at 206 °C. **Figure 3a** shows the DSC plot of the four polymorphs indicating that FI melts at 214.8 °C. FII gives two overlapping endothermic events, one peaking at 213 °C and the other at 214 °C, suggesting that FII converts to FI before melting. This has not been previously described in the literature. FIII shows a clear recrystallization peak at 196 °C and then melts at 214.5 °C, also suggesting a conversion to FI. This suggests that FI is the kinetically controlled, high energy phase, in line with the literature.[14] FIV loses water at 96 °C and then melts at 211 °C. **Figure 3b** shows the DSC thermograms of FII performed at a heating rate of 100 °C/min. On heating (H1) two endotherms are observed at 200.5 and 215.5 °C that are assigned to the polymorphic transformation of FII to FI followed by the melting of FI, respectively. On cooling from the melt (C1) an exothermic crystallization peak is observed at 180 °C. On reheating (H2) only one endotherm is observed at 215.5 °C indicating crystallization of FI during cooling.

3.2.2 Terahertz time-domain spectroscopy: Terahertz time-domain spectroscopy probes phonon absorption. To see if the observed transformations are gradual or sudden re-

arrangements of atoms, we carried out temperature-dependent terahertz spectroscopy. **Figure 4a** shows that FI does not change over the whole temperature range, confirming that it is the structure stable at high temperature. In contrast to the DSC analysis, conversion of FIII to FI could not be observed on heating up to the maximum accessible temperature (**Figure 4b**). The maximum temperature at which terahertz spectra could be recorded was 480 K (207 °C). As this is only slightly above the transition temperature observed by DSC it is likely that poor heat transfer between PTFE and diflunisal in the sample pellet is the reason for the failure to observe the FIII→FI conversion. **Figure 4c** shows that FIV very gradually starts converting to FI at 440 K (167 °C). Very recently Zhang *et al*. (Zhang, Wang, Tominaga, & Hayashi, 2016) published the mode analysis of FI and FIII, using the chirality of the molecules in the unit cell as a basis. This study suggests that both of these polymorphs have similar vibrational characteristics below 200 cm^{-1} and have significant contributions from the coupling of inter- and intramolecular modes. Both forms have two molecules in the unit cell and in the case of FI, the two molecules are symmetrically equivalent, while in FIII they are not, giving rise to non-identical phonon modes. One may note that while the terahertz spectra reported by Zhang show very sharp absorption features, it is not so in our case. This is predominantly due to the thermal broadening of the spectral peaks as well as the use of PTFE as a diluent. While PTFE is not an ideal diluent for terahertz spectroscopy as it may cause scattering effects, it has been chosen over other diluents as it allows measurements up to 500 K. Despite these effects, the terahertz spectra reported here have sufficient spectral resolution to observe and distinguish different polymorphs of diflunisal.

3.3 Milling induced phase transformations

3.3.1 Room temperature ball milling: XRPD patterns and Raman spectra of the milling experiments are shown in **Figures S4** and **S5** (SI). On milling for 30 minutes all polymorphs converted to FIII. This suggests that FIII is the thermodynamically stable structure. However, in the case of FI, FIII converts back to FI, when milling is continued for 120 min. **Figure S5a** shows the Raman spectral changes in the H-bonded C=O stretching region.

3.3.2 Cryogenic ball milling: Cryomilling of FI, FII and FIII for 60 min resulted in X-ray amorphous diflunisal (FA, **Figures 5, S6 and S7**). The three FA obtained from the different polymorphs were then subjected to accelerated temperature and humidity stress testing. Separate samples were placed in an oven at 60 °C for 2 hrs, in vacuum for 2 hrs and at 25 and 95 % relative humidity. Similar tests on other systems have been reported (SHOZO MIYAZAKI, 1976). FA produced from all of the polymorphs crystallized to FI (**Figures S6 and S7**), suggesting that FI is the easily accessible high energy state, as per Oswald's rule of stages. (Nývlt & Republic, 1995)

3.3.3 Liquid assisted grinding: LAG experiments were carried out using various solvents. Solvents like chloroform, tertrahydrofuran (THF) and valeric acid resulted in FIV solvates

(**Figure 6**). Ethanol, methanol, acetone, toluene and water gave FIII **(Figures 6 and S12)**. The formation of FIII on milling in the presence of traces of toluene is noteworthy, as solution crystallization from toluene yields FI. Similarly, water and acetone normally yield FIV solvate structures, while in the LAG experiments they seem to act as lubricants and lead to the thermodynamically stable FIII.

3.4 Humidity induced transformations

Another important factor during the processing of drugs is their stability under varying humidity conditions. All four polymorphs were placed in 95 % relative humidity chambers. FI, FIII and FIV were stable for 24 hrs, while FII converted to FIII as evident from the XRPD pattern (**Figure S9**). This may be explained by the fact that FII and III have very similar intermolecular interactions as discussed earlier, making the pathway for transformation easier than in the case of other polymorphs.

3.5 Crystallization from the melt

Melt quenching is often used as a technique to produce glasses, but in cases of fast crystallizers like diflunisal, this often results in the highest energy phase following Ostwald's rule of stages. We have observed that some parts of the melt started crystallizing even before it was immersed in liquid nitrogen. The H-bonded carbonyl region in the Raman spectrum of melt-quenched FI (**Figure S10**) suggests that the H-bonding pattern of the crystallized melt is very much similar to FI. However, while peaks at 783 and 683 cm^{-1} in the IR spectrum of melt-quenched FI (**Figure 7b**) are in agreement with this, a shoulder at 848 cm^{-1} also suggests the presence of FIV. The features around 1096 cm^{-1} suggest the presence of both FI and FIV. The XRPD pattern (**Figure 7a**) indicates the presence of FIV but some FI cannot be excluded. Fast crystallization possibly gives rise to FI, while liquid nitrogen may act as a solvent in crystallizing the remaining melt into FIV. Another possibility is that FIV is formed initially and the liquid nitrogen temperature arrests its conversion to FI.

3.6 Sublimation

Sublimation is a technique often used as a recrystallization method to remove impurities. In the absence of any template, it invariably results in the high energy metastable phase. Sublimation of diflunisal resulted in FI, which is the high temperature metastable state. The XRPD pattern is shown in **Figure S11**. We have previously used polymorph templates to control the selective crystallization of carbamazepine polymorphs from the gas phase. (Kamali

et al., 2016) Similar templating experiments with diflunisal were unsuccessful and only resulted in FI.

3.7 Order of polymorph stability

The observed phase transformations give insight into the stability order of the four polymorphs of diflunisal. With all forms converting to FI at high temperature, it is safe to say that FI is the high temperature metastable form. As all the forms resulted in FIII on milling, FIII can be assigned as the thermodynamically stable form. The packing coefficients computed for FI and FIII (with disorder removed from FI) of 70.4 and 72.9 % respectively also support this stability order. The only technique by which FIV *sans* solvent molecules in its channels can be produced is by melt-quenching, along with FI, suggesting that this form is probably formed as the first kinetic product according to Oswald's rule of stages. The presence of solvent in the channels is known to give up to 9 kJ/mol added stability to structures, (Cabeza, Day, Motherwell, & Jones, 2007) making the FIV solvate more stable than bare FIV. FII is known to convert into FIII on milling and also under humid conditions, making it less stable than FIII. However, it also converts partially to FI as seen in the thermal analysis, making FII less stable than FI at higher temperatures. The stability order of diflunisal polymorphs was first deduced from solubility experiments in water at 30 °C and was found to be FII > FIII > FI.(Cotton & Hux, **1985**) This was before the existence of either the channel solvate FIV(Hansen et al., 2001) or the more recent hydrate(Sung et al., 2013) were known. The possibility that conversion to hydrate forms during the original solubility experiments could invalidate any stability order conclusions from solubility measurements has been raised. (Perlovich et al., 2002) The results reported here in contrast to the solubility based work suggest the order FIII > FI > FII, FIV. The relative stability of FII and FIV remains unclear and computational studies are currently on-going to establish the order of stability of these polymorphs.

4. Conclusions

In this paper we have carried out extensive spectroscopic and phase transformation studies on the non-steroidal anti-inflammatory drug diflunisal. It is often difficult to reliably identify the polymorphs formed by XRPD. Spectroscopy can provide a useful alternative. The H-bonding patterns of the four polymorphs of diflunisal have a major influence on the carbonyl stretching frequencies observed in their Raman spectra. These differences provide a reliable basis for the distinction of diflunisal polymorphs. FI and IV, both have disordered F atoms and are structurally very similar, resulting in similar Raman and IR patterns. FII and III have similar spectral features suggesting that their structures are closely related. The various phase transformations undergone by the polymorphs are summarized in Scheme 2.

FII, which has a higher intrinsic dissolution rate than FI and III, has generally been very elusive, with preparation of bulk quantities hampered by its rapid transformation into FIII. Fast evaporation of an ethanolic solution below 80 °C seems to be a reliable method for the production of bulk quantities of FII, especially. However, under high relative humidity conditions FII eventually converts to FIII.

Acknowledgements

This work was supported by Science Foundation Ireland under Grant No. [12/RC/2275] as part of the Synthesis and Solid State Pharmaceutical Centre (SSPC). ARP would like to acknowledge ICHEC, Irish HPC system for computing time on the condominium access (nuig02). ARP also acknowledges the RIA Charlemont grant for financial support of a research visit to the University of Cambridge.

Supporting Information

Additional X-ray powder patterns, near infrared spectral assignments, IR, NIR and Raman spectra.

References

Bag, P. P., Patni, M., & Reddy, C. M. 2011. A kinetically controlled crystallization process for identifying new co-crystal forms: fast evaporation of solvent from solutions to dryness. ***Cryst Engg Comm***, 13: 5650 - 5652.

Brittain, H. G., Elder, B. J., Isbester, P. K., & Salerno, A. H. 2005. Solid-state fluorescence studies of some polymorphs of diflunisal. ***Pharmaceutical Research***, 22(6): 999-1006.

Cabeza, A. J. C., Day, G. M., Motherwell, W. D. S., & Jones, W. 2007. Solvent inclusion in form II carbamazepine. ***Chemical Communications***(16): 1600-1602.

Coquerel, G. 2014. Crystallization of molecular systems from solution: phase diagrams, supersaturation and other basic concepts. ***Chemical Society Reviews***, 43: 2286 - 2300.

Cotton, M., & Hux, R. **1985**. ***Diflunisal. In: Analytical***

profiles of drug substances: London: Academic Press, Inc.

Cross, W. I., Blagden, N., Davey, R. J., Pritchard, R. G., Neumann, M. A., Roberts, R. J., & Rowe, R. C. 2003. A whole output strategy for polymorph screening: Combining crystal structure prediction, graph set analysis, and targeted crystallization experiments in the case of diflunisal. ***Crystal Growth & Design***, 3(2): 151-158.

Dharmendra Singhal, W. C. 2004. Drug polymorphism and dosage form design: a practical perspective. ***Advanced Drug Delivery Reviews***, 56(3): 335–347.

Friscic, T., Childs, S. L., Rizvi, S. A. A., & Jones, W. 2009. The role of solvent in mechanochemical and sonochemical cocrystal formation: a solubility-based approach for predicting cocrystallisation outcome. ***Crystengcomm***, 11(3): 418-426.

Hansen, L. K., Perlovich, G. L., & Brandl, A. B. 2001. The 1 : 1 hydrate of diflunisal. ***Acta Crystallographica Section E-Structure Reports Online***, 57: O477-O479.

Hao, H., Barrett, M., Hu, Y., Su, W., Ferguson, S., Wood, B., & Glennon, B. 2012. The Use of in Situ Tools To Monitor the Enantiotropic Transformation of p-Aminobenzoic Acid Polymorphs. ***Organic Process Research & Development***, 16(1): 35-41.

Jepsen, P. U., DTU Fotonik – Department of Photonics Engineering, T. U. o. D., 2800 Kongens Lyngby, Denmark, DTU Fotonik – Department of Photonics Engineering, T. U. o. D., 2800 Kongens Lyngby, Denmark, Cooke, D. G., DTU Fotonik – Department of Photonics Engineering, T. U. o. D., 2800 Kongens Lyngby, Denmark, Koch, M., & Fachbereich Physik, P. U. M., Renthof 5, 35032 Marburg, Germany. 2017. Terahertz spectroscopy and imaging – Modern techniques and applications. ***Laser & Photonics Reviews***, 5(1): 124-166.

Kamali, N., Erxleben, A., & McArdle, P. 2016. Unexpected Effects of Catalytic Amounts of Additives on Crystallization from the Gas Phase: Depression of the Sublimation Temperature and Polymorph Control. ***Crystal Growth and Design***, 16(5): 2492 - 2495.

Lee, E. H. 2014. A practical guide to pharmaceutical polymorph screening & selection. ***Asian Journal of Pharmaceutical Sciences***, 9(4): 163–175.

Macfhionnghaile, P., Hu, Y., Gniado, K., Curran, S., McArdle, P., & Erxleben, A. 2014. Effects of Ball-Milling and Cryomilling on Sulfamerazine Polymorphs: A Quantitative Study. ***Journal of Pharmaceutical Sciences***, 103(6): 1766-1778.

Martinez-Oharriz, M. C., Martin, C., Goni, M. M., Rodriguez-Espinosa, C., Tros-Ilarduya, M. C., & Zornoza, A. 1999. Influence of polyethylene glycol 4000 on the polymorphic forms of diflunisal. ***European Journal of Pharmaceutical Sciences***, 8(2): 127-132.

Nývlt, J., & Republic, I. o. I. C. A. o. S. o. t. C. R. P. P. C. 1995. The Ostwald Rule of Stages. ***Crystal Research and Technology***, 30(4): 443-449.

Pallipurath, A. R., Civati, F., Eziashi, M., Omar, E., McArdle, P., & Erxleben, A. 2016. Tailoring Co-crystal and Salt Formation and Controlling the Crystal Habit of Diflunisal. ***Crystal Growth and Design***.

Pallipurath, A. R., Skelton, J. M., Warren, M. R., Kamali, N., McArdle, P., & Erxleben, A. 2015. Sulfamerazine: Understanding the Influence of Slip Planes in the Polymorphic Phase Transformation through X-Ray Crystallographic Studies and ab Initio Lattice Dynamics. ***Molecular pharmaceutics***, 12(10): 3735-3748.

Patterson JE, J., ames MB, Forster AH, Lancaster RW, Butler JM, & T., R. 2005. The Influence of Thermal and Mechanical Preparative Techniques on the Amorphous State of Four Poorly Soluble Compounds. ***Journal of Pharmaceutical Sciences***, 94(9): 1998–2012.

Perlovich, G. L., Hansen, L. K., & Bauer-Brandl, A. 2002. Interrelation between thermochemical and structural data of polymorphs exemplified by diflunisal. ***Journal of Pharmaceutical Sciences***, 91(4): 1036-1045.

SHOZO MIYAZAKI, M. N., TAKAICHI ARITA. 1976. Polymorphic Transformation of Chlortetracycline Hydrochloride Crystals Studied by Infrared Spectrophotometric Method. ***Chemical and Pharmaceutical Bulletin***, 24(8): 1832 - 1838.

Shuang Chen, Ilia A. Guzei, a., & Yu*, L. 2005. New Polymorphs of ROY and New Record for Coexisting Polymorphs of Solved Structures. ***JOurnal of American Society***, 127(27): 9881 - 9885.

Socrates, G. 2001. ***Infrared and Raman Characteristic Group Frequencies: Tables and Charts***. London.

Srirambhatla, V. K., Guo, R., Price, S. L., & Florence, A. J. 2016. Isomorphous template induced crystallisation: a robust method for the targeted crystallisation of computationally predicted metastable polymorphs. ***Chemical Communications***, 52: 7384 - 7386.

Sung, H.-L., Fan, Y.-L., Yeh, K., Chen, Y.-F., & Chen, L.-J. 2013. A new hydrate form of diflunisal precipitated from a microemulsion system. ***Colloids and Surfaces B-Biointerfaces***, 109: 68-73.

Yihong Qiu, Y. C., Geoff G.Z. Zhang. 2009. ***Theories and Techniques in the Characterization of drug substances and excipients***.

Zhang, F., Wang, H.-W., Tominaga, K., & Hayashi, M. 2016. Characteristics of Low-Frequency Molecular Phonon Modes Studied by THz Spectroscopy and Solid-State ab Initio Theory: Polymorphs I and III of Diflunisal. ***The Journal of Physical Chemistry B***, 120(8): 1698 - 1710.

Schemes:

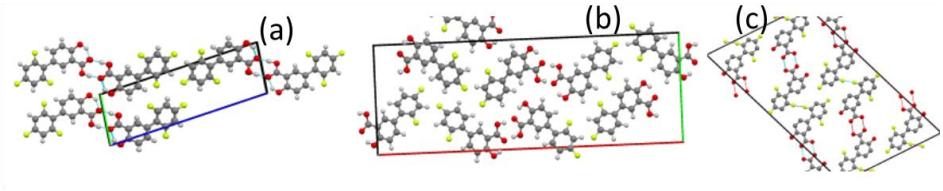

Scheme 1. Interactions in the polymorphs of diflunisal, (a) FI (FAFWIS01), (b) FIII (FAFWIS02), and (c) FIV (FAFWIS).

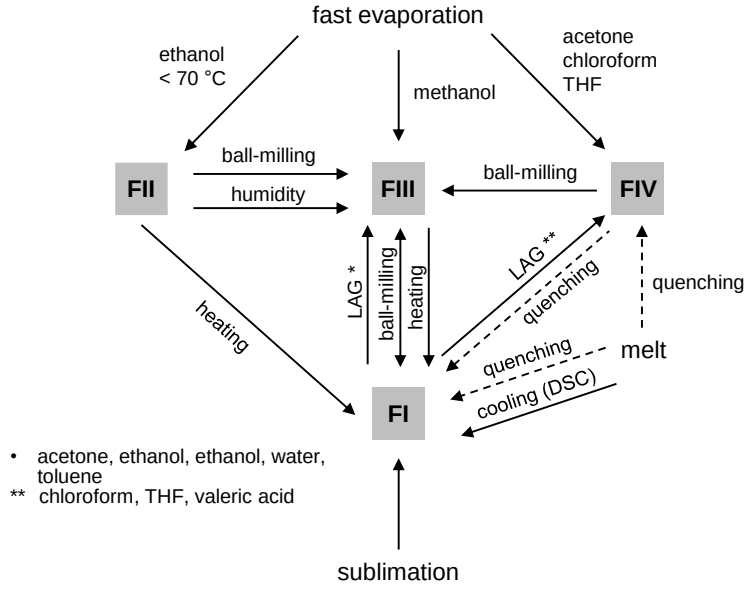

Scheme 2. Phase transformations of diflunisal polymorphs under various conditions. The dashed arrows indicate that the pathway cannot be unambiguously assigned.

Figures

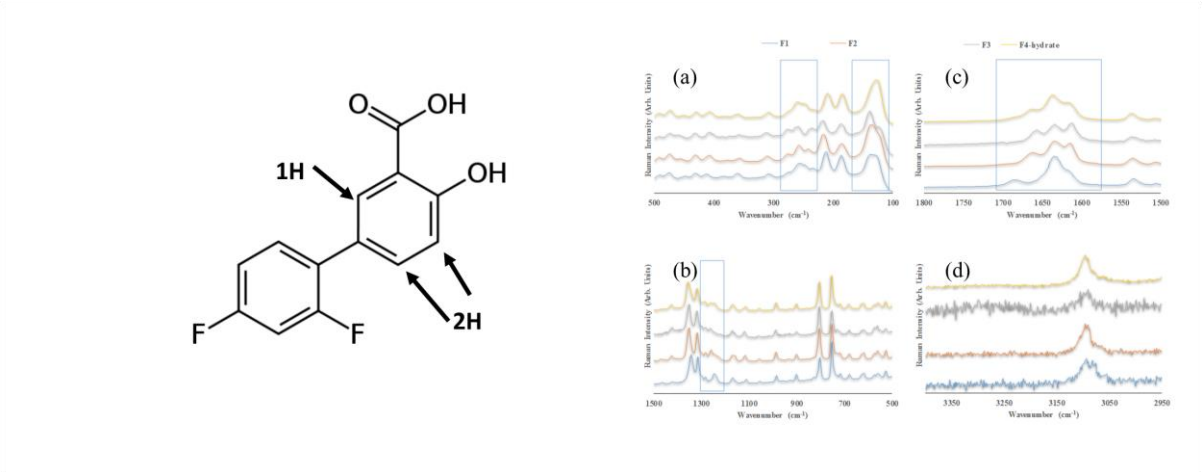

Figure 1. Molecular structure of diflunisal, with the positions of the carbon atoms in the 1,2,4 tri-substituted ring denoted as 1H and 2H (left) and different wavenumber ranges of the Raman spectra of the four polymorphs (right). The areas highlighted inside blue boxes are the peaks that are influenced by the structural differences in the polymorphs, i.e. the nature and strength of H-bonding.

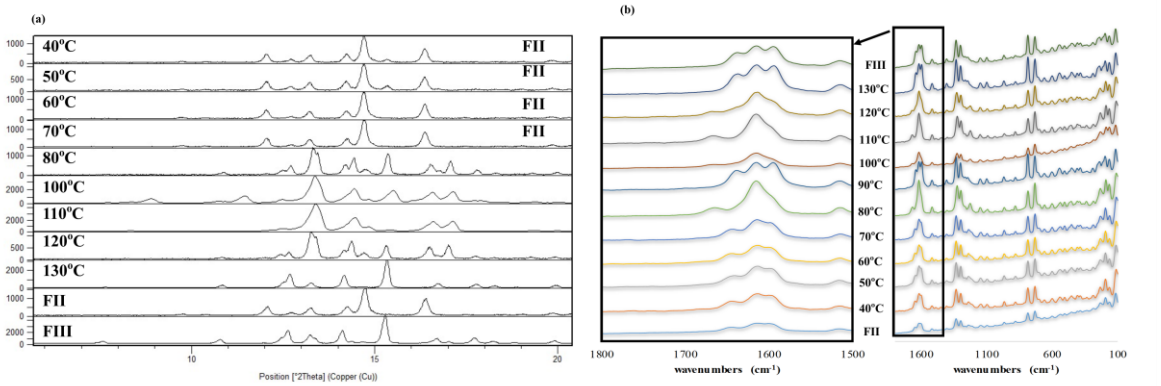

Figure 2. (a) X-ray powder diffraction patterns and (b) Raman spectra of diflunisal polymorphs obtained by fast evaporation of ethanol at various temperatures. The inset in (b) shows the carbonyl region of the Raman spectra, expanded for clarity. Both techniques show the formation of FII between 40 ºC to 70 ºC, and FI or FIII at higher temperatures.

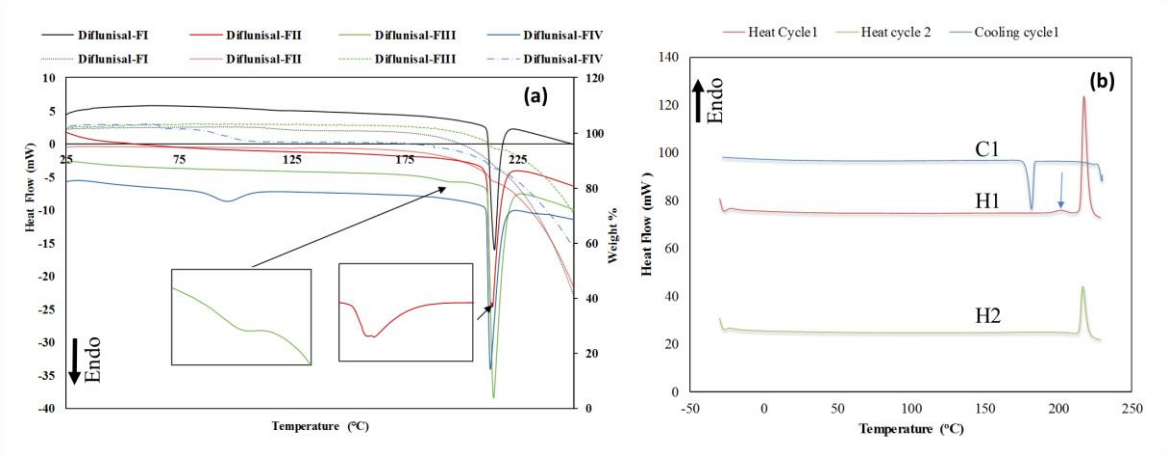

Figure 3. Thermal analysis of the polymorphs of diflunisal. (a) Solid lines represent differential scanning calorimetry (DSC) and the dotted lines represent thermogravimetric analysis (TGA) at 10 ºC/min heating rate. The inset in green shows the recrystallization event of FIII to FI. The inset in red shows the double peak in the case of FII. (b) DSC of FII run at 100 ºC/min (H1), followed by a cooling cycle (C1) and a reheating cycle (H2).

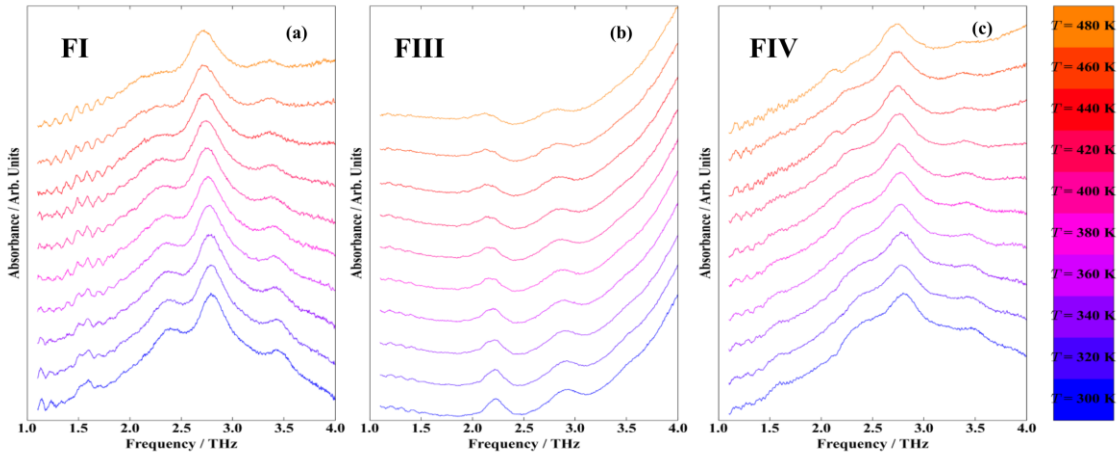

Figure 4. Terahertz time-domain spectroscopic analysis of the polymorphs of diflunisal. (a) FI, (b) FIII, and (c) FIV (obtained from acetone and water). FIV converts to FI at 167 °C (440 K). The colour of the spectra denotes the temperature at which the spectra were obtained.

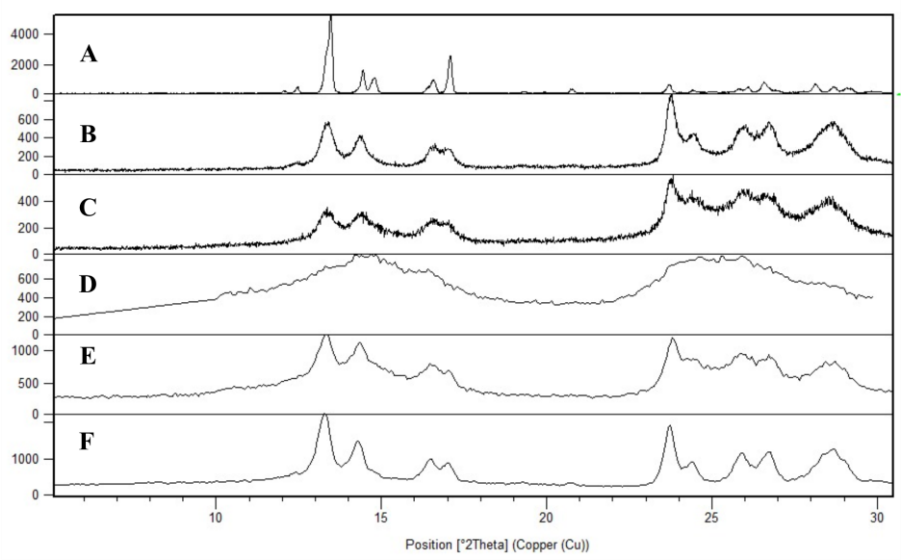

Figure 5. X-ray powder diffraction patterns of (A) FI, (B) FI cryomilled for 60 min and kept under vacuum for 2 hrs, (C) FI cryomilled for 60 min and kept at 60 ºC for 2 hrs, (D) FI cryomilled for 60 min, (E) FI cryomilled for 60 min and kept at 25% relative humidity and (F) FI cryomilled for 60 min and kept at 95% relative humidity. All patterns show ageing and formation of FI.

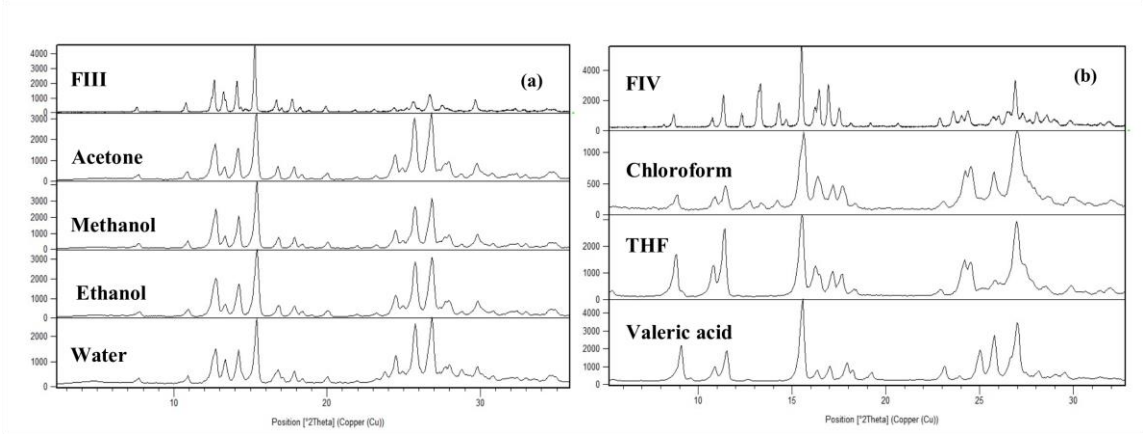

Figure 6. X-ray powder diffraction patterns of diflunisal polymorphs obtained from liquid assisted grinding of FI with (a) acetone, methanol, ethanol and water showing the formation of FIII and (b) with chloroform, terahydrofuran (THF) and valeric acid showing the formation of FIV channel solvates.

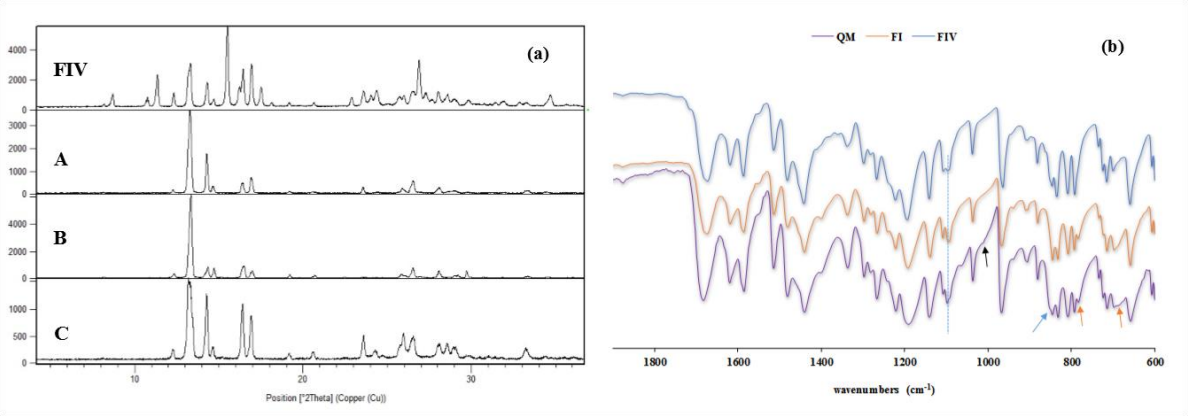

Figure 7. X-ray powder diffraction patterns of FIV and melt-quenched FI (A), FII (B) and FIII (C); (b) Mid-IR spectra of melt-quenched FI, pure FI and FIV showing the presence of both FI and FIV in the melt-quenched sample.

Table 1. Raman Spectral Assignments of Peaks That Are Distinct in the Four Different Polymorphs of Diflunisal

FI	**FII**	**FIII**	**FIV**	**Assignments**
126 132 181 204 234 243 250 273	118 (sh) 142 183 211 238 254 270	121 137 186 213 234 254 275	123 181 204 229 243 263	Phonon region
708	712 727	712 718	708 725	Out-of-plane CH deformation in trisubstituted benzenes, normally associated with the presence of halogen substitution.
1230	1221 1235 1250	 1250	 1230 1252	CH in-plane deformations
1275	1271	1273 1292	1273	O-H deformation in COOH monomers
1611 1629	1611 1629	1610 1629	1611 1631	C=O stretching in aromatic COOH with ortho-OH
1685	1658	1651	1665	C=O stretches involved in intra-molecular H-bonding interactions

Table 2. IR Spectral Assignments of the Four Polymorphs of Diflunisal

FI	FII	FIII	FIV	Assignments
	649	649		Out-of-plane deformation (2H) in 1,2,4-trisubstituted benzene rings
	670	670		
698	702	702	700	
714	718	718	716	
728			735	
	894	895		Out-of-plane deformation (1H) in 1,2,4-trisubstituted benzene rings.
1096			1095	C=C stretching in asymmetrically substituted benzene rings
	1207	1208		
1298	1329	1329	1297	OH deformations
	1376	1376		COH bending in OH groups associated with C=O groups through H-bonding
1400	1409	1409	1410	
2546	2532	2532	2531	OH stretch in intra-molecular H-bonded o-substituted carboxylic acid
2566	2561	2561		
2603	2623	2618		
2872	2862	2862	2867	OH stretch in associated carboxylic acid
	2940	2949		Aromatic C-H stretch
	2991	2986		
3075	3052	3063	3077	
	3262	3262		OH stretch in associated carboxylic acid
1877			1876	C-H out-of-plane deformation, overtones and combination bands
	1908	1905		
		1927		
	1934	1937	1941	
1980		1980	1977	
			1990	

Table of Contents Graphic